富山大学水素同位体科学研究センター研究報告27：17－26，2007.

Isotope Effect on Methane Decomposition observed between CH_4 and CD_4 over Zr

K. Watanabe, W. Shu* and M. Matsuyama
Hydrogen Isotope Research Center, University of Toyama
Gofuku 3190, Toyama 930-8555, Japan
* Present Affiliation: ITER International Organization, Tritium Plant Group
(Received January 12, 2008: accepted March 12, 2008)

ABSTRACT

The decomposition of methane and deutero-methane (CD_4) over Zr, Zr_4Ni and Zr_2Ni was investigated to develop highly active materials for capturing tritiated methane inevitably formed in tritium handling systems. None of the decomposition or absorption curves could been described by any simple kinetic equations appearing in the literature. They could be described by a series reaction scheme including growth of carbonaceous deposits on the surface. The reaction mechanisms were studied in more detail in the present study, and it was revealed that the absorption/decomposition of methane proceeds via the steps $CH_4(g) \xrightarrow{k_1} CH_3(a) \xrightarrow{k_2} CH_2(a) \xrightarrow{k_3}$ C-deposits.

The kinetic isotope effect on the decomposition/absorption of CH_4 and CD_4 was also analyzed for Zr in the light of *ab initio* calculations using small clusters including two or three Zr atoms.

1. Introduction

Tritiated methane is one of the most important impurities in the tritium gas used in a variety of tritium handling facilities including tritium processing systems of thermonuclear fusion reactors. This is because the tritium gas is contaminated by many impurity gases (including tritiated methane) generated during tritium handling and tritiated methane is one of the most hazardous material for human safety and living environments. Accordingly extensive studies have been done for removing tritiated methane from the contaminated tritium gas. The most typical way so far developed is catalytic oxidation to produce tritiated water. But this method produces a large amount of tritiated waste water and gives rise to problems such as its storage and/or detritiation of the waste water.

An attractive alternative way is the utilization of a kind of metallic compounds known as getters for vacuum technology. The present authors have developed promising metallic compounds consisting of Zr and a transition element of the group VIII, among which the compounds consisting of Zr and Ni are found to be most beneficial for tritium handling[1]. They can easily absorb tritium not only in the elemental form but also in the form of water, ammonia and gaseous hydrocarbons as well as non-radioactive impurity species such as CO, CO_2, O_2 and N_2. Especially they could decompose and absorb methane that is most inactive

substance among the impurity gases. They work at relatively low temperature in comparison with other gettering materials[2, 3].

In the previous paper, methane (CH_4) absorption curves for Zr, Zr_4Ni and Zr_2Ni were analyzed by assuming sequential removal of hydrogen atoms from methane and it was found that the sequential kinetic equations consisted of three elementary reactions as $CH_4(g) \xrightarrow{k_1} CH_3(a) \xrightarrow{k_2} CH(a) \xrightarrow{k_3}$ C-deposits could reproduce the absorption curves of CH_4 rather well down to 0.1% of the initially loaded amount.

The present paper describes further details of kinetic analysis of the absorption curves and a model for understanding the kinetic processes of methane absorption by Zr in the light of *ab inito* calculations for samll clusters concerning the methane decomposition on Zr(1000) surface. Discussion is also made for the kinetic isotope effect observed for CH_4 and CD_4 decomposition/absorption over/by Zr.

2. Experimentals

Although the experimental apparatus, procedures and results obtained with Zr and Zr-Ni alloys have been described in previous papers[1, 4, 5], a brief description of experimental procedures is given below for readers convenience.

The sample materials concerned with the present paper is Zr. It was used as powder of 200 mesh (below 74 μm). According to BET measurements using Kr, the specific surface area was 0.08 m^2/g. Decomposition/absorption curves of methane and deutero-methane (CD_4) on Zr surface was measured by constant volume method, and the absorption curves were given by the pressure as a function of time, $P(t) - t$, where 0.5 grams of powder were used. Prior to the absorption measurements, the sample powder was heated at 423 K for 2 hours under vacuum and then at 873 K for 2 hours as the standard activation procedures in the apparatus whose residual pressure was routinely below 2.67×10^{-6} Pa.

The absorption curves were measured by setting the initial pressure at 13.3 Pa in the reaction cell of 173 cc.

3. Kinetic Model

In the previous paper[6], the absorption curves of methane over Zr and Zr-Ni alloys were analyzed by accounting two dimensional potential energy surface (PES) calculated by using the Gaussian 03 package[7]. On account of the results of PES calculations, it was assumed that the absorption of methane by Zr and Zr-Ni alloys proceeds via the elementary reactions as

$$CH_4(g) + 2\,S \xrightarrow{k_1} \underset{n(CH_3)}{S\text{-}CH_3(a)} + \underset{n(H)}{S\text{-}H(a)} \tag{1}$$

$$S\text{-}CH_3(a) + 2\,S \xrightarrow{k_2} \underset{n(CH)}{S\text{-}CH(a)} + 2\,S\text{-}H(a) \tag{2}$$

$$2\ \text{S-CH}(a) \xrightarrow{k_3} \underset{n(cd)}{\text{S-CH}_n(a)}, \tag{3}$$

where S denotes a vacant site for adsorption of respective species, S-R (where R = H, CH, CH_3) adsorbed species, and n the amount of adsorbed species indicated in parentheses; k_1, k_2 and k_3 are the respective rate constants.

In addition, it was assumed to reproduce the tailing part of absorption curves that carbonaceous products formed via reaction (3) grows spherical-segmentally and its surface coverage can be described by the term $n_{cd}^{3/2}$, where n_{cd} denotes the number of mols of the carbonaceous deposits. Accordingly the kinetic process was described as [1)]

$$-(\frac{n_{\text{CH}_4}}{d\,t}) = k_1 n_{CH_4}(s_0 - n_{CH_3} - n_{cd}^{3/2})^2 \tag{4}$$

$$(\frac{n_{CH_3}}{d\,t}) = (k_1 n_{CH_4} - k_2 n_{CH_3})(s_0 - n_{CH_3} - n_{cd}^{3/2})^2 \tag{5}$$

$$(\frac{n_{CH}}{d\,t}) = k_2 n_{CH_3}(s_0 - n_{CH_3} - n_{cd}^{3/2})^2 - k_3 n_{CH}^2, \tag{6}$$

where s_0 represents the number of active sites on the surface and n_X denotes the number of molecules of species X (X = CH_4, CH, or C).

These equations could reproduce well the observed absorption curves of CH_4 over Zr, Zr_4Ni and Zr_2Ni. However, more detailed examination of transition states in each elementary reaction revealed that reaction (2) is not likely to occur. Instead, it is more plausible that the adsorbed $CH_3(a)$ decomposes to produce $CH_2(a)$ and $H(a)$. It suggests that one vacant site adjacent to $CH_3(a)$ is enough for the decomposition. On account of this situation, the reaction mechanism should be described as

$$\text{CH}_4(g) + 2\ \text{S} \xrightarrow{k_1} \underset{n(CH_3)}{\text{S-CH}_3(a)} + \underset{n(H)}{\text{S-H}(a)} \tag{7}$$

$$\text{S-CH}_3(a) + \text{S} \xrightarrow{k_2} \underset{n(CH_2)}{\text{S-CH}_2(a)} + \text{S-H}(a) \tag{8}$$

$$2\ \text{S-CH}_2(a) \xrightarrow{k_3} \underset{n(cd)}{\text{S-CH}_n(a)}. \tag{9}$$

Accordingly the kinetic equations should be revised as

$$-(\frac{n_{\text{CH}_4}}{d\,t}) = k_1 n_{CH_4}(s_0 - n_{CH_3} - n_{cd}^{3/2})^2 \tag{10}$$

$$(\frac{n_{CH_3}}{d\,t}) = [k_1 n_{CH_4}(s_0 - n_{CH_3} - n_{cd}^{3/2}) - k_2 n_{CH_3})](s_0 - n_{CH_3} - n_{cd}^{3/2}) \tag{11}$$

$$(\frac{n_{CH_2}}{d\,t}) = k_2 n_{CH_3}(s_0 - n_{CH_3} - n_{cd}^{3/2}) - k_3 n_{CH_2}^2, \tag{12}$$

where it is assumed that $CH_2(a)$ further decomposes to $CH(a)$ and $C(a)$ and they combine together to form carbonaceous deposits. It is also supposed that the coverage of $CH_2(a)$ is

[1)] Eqns.(29), (30) and (31) in the previous paper[6] should be read as Eqs.(4), (5) and (6) in this paper. They were mistyped.

negligible in comparison with other adsorbed species. This is the similar assumption made for $CH(a)$ in the previous paper.

4. Results and Discussion

4.1. Analysis of Absorption Curves

Figures 1 and **2** shows the absorption curves over Zr for CH_4 and CD_4 , respectively, at different temperatures, where the dots represent the observed values and solid lines are calculated results by using the estimated rate constants obtained by trial-and-error fitting procedures. The details of the fitting has been described previously[6]. It is seen in these figures that all of the absorption curves could be reproduced quite well by the revised kinetic equations described above. It should be noted that the absorption curves of CH_4 could be reproduced equally well by the preceding equations with the second order dependence for the second step decomposition of $CH_3(a)$, Eq.(5)[6].

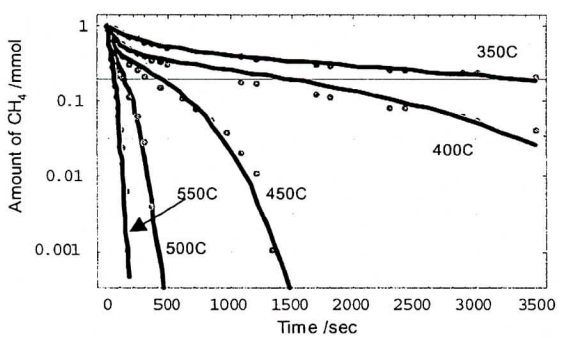

Fig. 1. Absorption curves of CH_4 for Zr at 350, 400, 450, 500 and 550 ℃

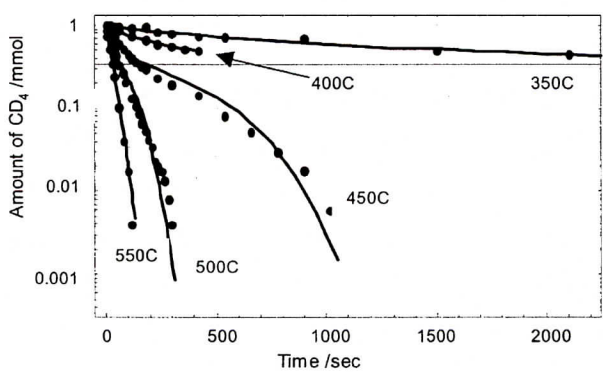

Fig. 2. Absorption curves of CD_4 for Zr at 350, 400, 450, 500 and 550 ℃

Neglection of diffusion processes in the kinetic model is justfied by considerably fast diffusion of hydrogen and and slow diffusion of carbon in Zr; the diffusion constants are reported to be 10.0×10^{-3} Exp$[-49.2 \times 10^3/RT]$[8] and 3.5×10^{-5} Exp$[-128 \times 10^3/RT]$[9] for hydrogen and carbon, respectively, where the frequency factor is in cm^2/scc. and the activation energy in kJ/mol. It is demonstrated in **Figs. 3** and **4** by plotting the change in the depth profiles of hydrogan at 350 and carbon at 550 ℃, respectively, with time. The diffusion profiles were calculated for the infinte media by assuming that the initial depth profiles of hydrogen and carbon were given by a step function with the unit concentration in a region of $-a < x < a$, where a was set to 100 Å thickness, and the concentration is null outside of this region. The solution of the differentail equation is given by $c[x,t] = (1/2)\{\mathrm{erf}\,[(a-x)/(2\sqrt{D\,t})] + \mathrm{erf}\,[(a+x)/(\sqrt{D\,t})]\}$[10]. In this case, the center of the media could be considered as the surface. Then the abscicca is the depth from the surface, which is measured in cm, and the ordinate the

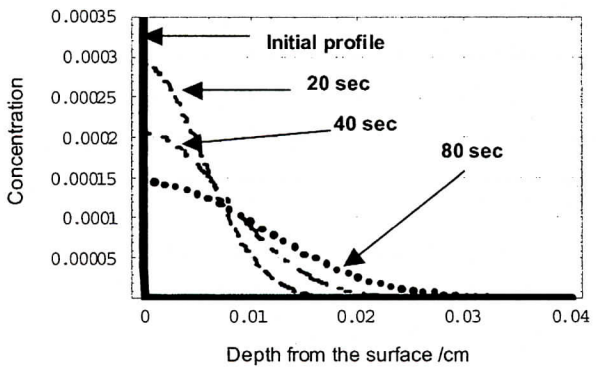

Fig. 3. Change in hydrogen depth profile with time at 350 C

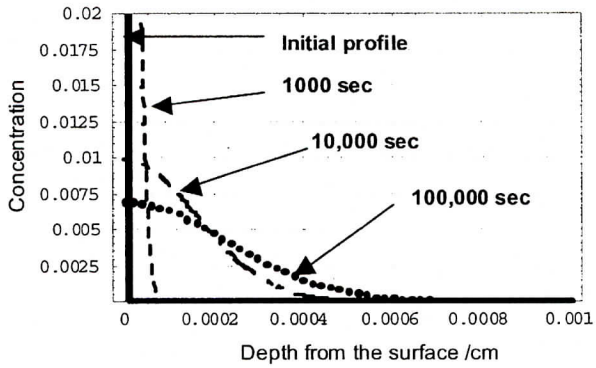

Fig. 4. Change in carbon depth profile with time at 550 ℃

concentraion of H or C in **Figs.3** and **4**. It is seen in **Fig.3** that the hydrogen concentration in the top-most region decreases to 0.0003 in 20 seconds and it is reduced to it's half in 80 seconds at 350 ℃. It is also noticed that the front of the depth-profile is extended to 0.035 cm from the surface. These features indicate that the diffusion of hydrogen, which is formed by the step-wise decomposition of methane, is extremely fast even at the lowest temperature adopted in the present study. Evidently hydrogen diffuses into bulk to be rapidly removed from the surface and then the hydrogen diffusion does not take part in the kinetic equations. The diffusion of carbon is, on the other hand, remarkably slow as seen in **Fig.4**. At the highest temprature of the absorption measurement, 550 ℃, it takes 10^4 seconds for the carbon concentration in the top-most region to be reduced to one hundrendth of the initial value. It is also seen that it takes 10^5 seconds for the front of the diffusion profile to appear at the depth of 0.0007 cm, which is about one tenth of the diameter of Zr-particles used in the present study. All of these features clearly indicate that the diffusion of carbon into the bulk does not take place under the present experimental conditions and then it could be certainly excluded from the kinetic equations.

4.2. Temperature Dependence of the Rate Constants

Figure 5 shows the Arrhenius plots of the rate constants, k_1, of CH_4 and CD_4 obtained for Zr, where the abscissa is the rate constant in $1/sec.mmol^2$ and the ordinate is the reciprocal temperature. It can be seen that the rate constants for CH_4 and CD_4 gave rather good linear straight lines. The activation energies were determined to be 72.0 and 79.7 kJ/mol for CH_4 and CD_4, respectively. The respective frequency factors were

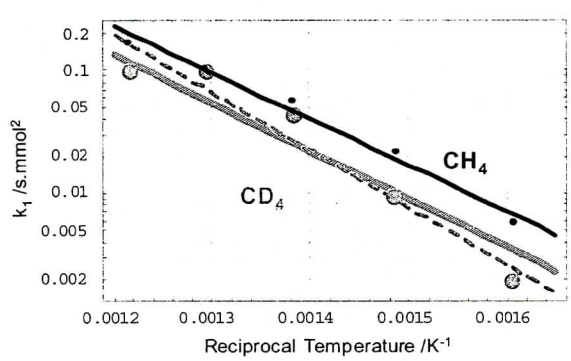

Fig. 5. Arrhenius plots of k_1 for CH_4 and CD_4 over Zr

evaluated to be 7.4×10^3 and 8.0×10^4 for CH_4 and CD_4 [1/sec.mmol^2], respectively. The difference in the activation energy was 7.7 kJ/mol, whereas the ratio of the frequency factors, ν_{CH_4}/ν_{CD_4}, was 0.09.

Figures 6 and **7** compare the rate constants, k_2 and k_3, between CH_4 and CD_4, where the abscissa is in 1/sec.mmol scale. It is noted that the data points of k_2 and k_3 for CD_4 at 400C were excluded for making Arrhenius plots, because the data points were not taken for a period enough long time to determine these rate constants. It is seen in these figures that in these cases the data points scattered largely in comparison with those for k_1. Especially the scattering was significant for k_2. This is because k_2 mainly concerns with the first inflecting concave part of the absorption curves, and k_3 does the second inflection convex part accelerating the absorption in the end of the absorption curves. It was rather difficult to evaluate their values in comparison with those of k_1. Nevertheless straight lines were drawn from these points, and the activation

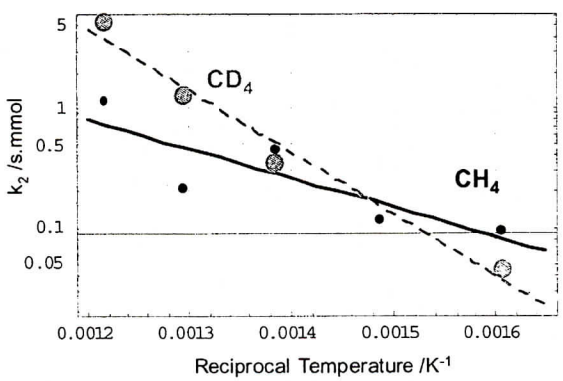

Fig. 6. Arrhenius plots of k_2 for CH_4 and CD_4 over Zr

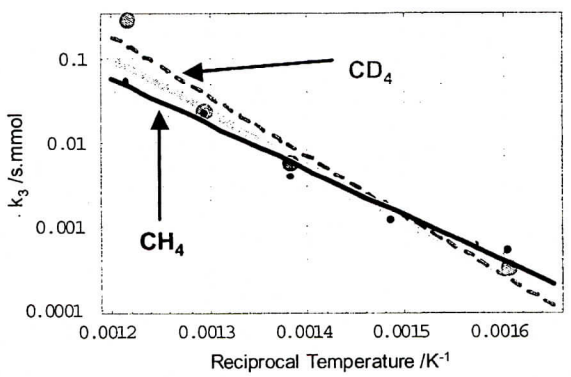

Fig. 7. Arrhenius plots of k_3 for CH_4 and CD_4 over Zr

energies were evaluated as 47.1 and 99.2 kJ/mol for $k_2(CH_4)$ and $k_2(CD_4)$, respectively, and 104 and 137 kJ/mol for $k_3(CH_4)$ and $k_3(CD_4)$, respectively. The activation energy for CH_4 was smaller than that for CD_4 in both of these cases. The differences in the activation energy were 52 kJ/mol for k_2 and 33 kJ/mol for k_3. These differences are unacceptably large as the kinetic isotope effect. In addition, it should be noted that the differences in the frequency factor are also significantly large. These points are discussed below in connection with the *ab initio* cluster calculations.

4.4. Isotope Effect examined by *ab initio* Calculation

The kinetic isotope effect observed for methane decomposition on Zr was examined by use of the Gaussian-03 package[7]. The *ab inito* calculations were carried out for small clusters containing two or three Zr-atoms on the Zr(1000) surface. Then the distance between Zr-atoms was set to 3.2311 Å[11]. **Figure 8** illustrates a cluster consisting of two Zr-atoms and a CH_4 molecule that was given as the activated complex for adsorption of CH_4 molecules on the Zr surface. The distance between Zr(1) and C(3) is 2.371 and that between C(3) and H(4,5,7) is

1.10 Å that is almost equal to the bonding distance of C-H in a methane molecule. On the other hand, the C(3)-H(6) distance is elongated to 1.375 Å and the displacement vector for the imaginary vibration is directed toward the second Zr atom, Zr(2). **Figures 9, 10 and 11** illustrate adsorbed $CH_3(a)$, activated complex for $CH_3(a)$ decomposition and product of the decomposition, respectively.

In these cases, the cluster models consisting of three Zr atoms were adopted, because the models consisting of two Zr atoms could not afford meaningful imaginary frequency for the activated complex. According to the models of adsorbed $CH_3(a)$ for three Zr atom system shown in **Fig.9**, the distance between C-Zr(2) is 2.212 Å. The bonding distance of C-H(4,5,7)

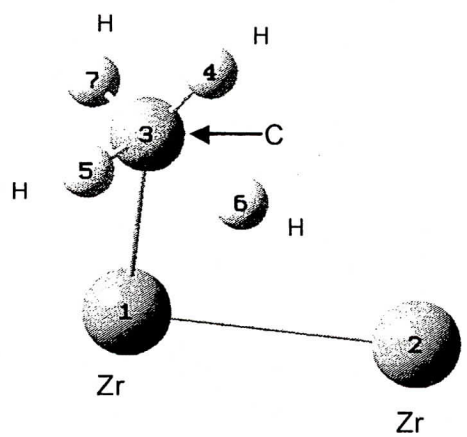

Fig. 8. Structure of the activated complex for methane decomposition obtained for a cluster consisting of two Zr atoms

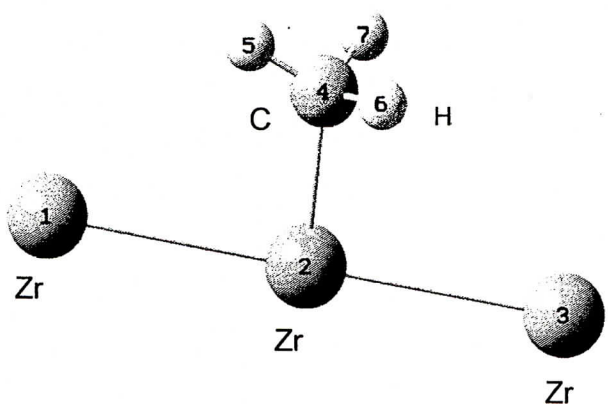

Fig. 9. Structure of adsorbed $CH_3(a)$ obtained for a cluster consisting of three Zr atoms

in the adsorbed $CH_3(a)$ is almost the same at 1.100 Å as that for adsorbed $CH_3(a)$. With respect to the activated complex for decomposition of the adsorbed $CH_3(a)$ shown as **Fig.10**, the Zr-C distance is reduced to 2.065, whereas that of C-H(5,7) is kept almost the same at 1.100 Å, but the length of the breaking bond of C-H(6) is 1.706 Å, where the displacement vector of imaginary vibration is directed toward Zr(1). As for the reaction product seen in **Fig.11**, the bonding lengths of Zr(2)-C and Zr(2)-H(8) are 2.265 and 1.988 Å, respectively.

The activation energies for $CH_4(g)$ decomposition/adsorption and for $CH_3(a)$ decomposition/adsorption to $CH_2(a)$ are evaluated to be 199.7 and 95.3 kJ/mol, respectively, that were calculated from the energies of bottoms of the potential wells; that is, the classical energy difference. These values are too large in comparison with those obtained from the experimental data. As mentioned in the previous paper[6], these large discrepancies should be ascribed to the over-simplification of the cluster models. Nevertheless the simplified cluster models could give some insight into the isotope effect on k_1, k_2 and k_3 for the decomposition over Zr surface. According to the calculation, the difference in the activation energy for k_1 between CD_4 and CH_4 was evaluated to be 4.8 kJ/mol.

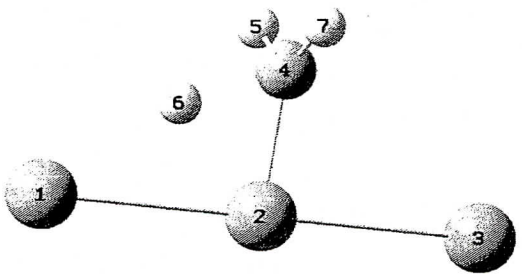

Fig. 10. Structure of activated complex for the decomposition of $CH_3(a)$ obtained for Zr3-cluster model

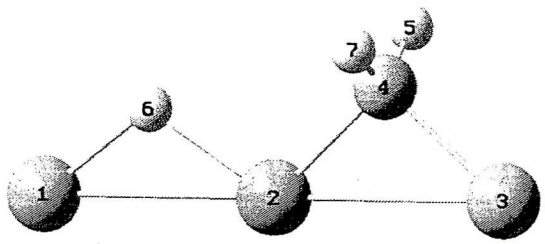

Fig. 11. Product of the decomposition of $CH_3(a)$ for Zr3-cluster

This value agrees rather well to the value of 7.7 kJ/mol obtained from the fitting of the experimental data. With respect to the frequency factor, the frequency ratio of $k_{01}(CH_4)/k_{01}(CD_4)$ can be estimated from the imaginary frequency ratios as the high temperature limit from $\nu^*(CH_4)/\nu^*(CD_4)$ [12]. The observed ratio of about 0.1 is far smaller than the value of 1.37 calculated from $\nu^*(CH_4)/\nu^*(CD_4)$. But it should be accounted that the determination of the frequency factor from Arrhenius plots is a troublesome problem, especially in the case that only a limited numbers of experimental data is available as in the present study. This is demonstrated in **Fig.5** by the gray thick line which was drawn by assuming $k_{01}(CD_4) = k_{01}(CH_4)/1.37$.

With respect to k_3, it is expected that there appears no noticeable isotope effect because this step is considered to correspond to the accumulation of adsorbed species as $CH_2(a)$, $CH(a)$ and/or $C(a)$ to form carbonaceous deposits on the surface. Accordingly **Fig.7** should be read as the plots for $k_3(CH_4)$ and $k_3(CD_4)$ agrees each other. The gray thick line in **Fig.7** shows the least square fit for the data points of CH_4 and CD_4, which gave the activation energy of 124 kJ/mol.

As for k_2, almost the same consideration could be valid for the difference in the activation energy and the ratio of frequency factors as the consideration for the isotope effect on k_1. Namely, the difference in the activation energy was evaluated from the *ab initio* calculation as 3.69 kJ/mol and the ratio of the frequency factors was given as $\nu^*(CH_3)/\nu^*(CD_3) = 1.37$. From this viewpoint, the results shown in **Fig.6** are not physically meaningful. This is largely due to the difficulty for determining precise values from the limited number of absorption curves with enough accuracy. More data with higher accuracy are required to obtain reliable k_2. Concerning this point, Zr_2N showed much more plausible isotope effects and the analysis in combination with *ab initio* calculations will be presented in the next paper.

5. Conclusions

Absorption curves of CH_4 and CD_4 for Zr were analyzed by use of a series of kinetic equations

and the results of kinetic analysis were further inspected by taking account of *ab inito* calculations for small clusters consisting of two or three Zr atoms and methane by using Gaussian03 package.

It was found that the revised kinetic model accounting the sequential removal of hydrogen atoms as $CH_4(g) \xrightarrow{k_1} CH_3(a) \xrightarrow{k_2} CH_2 \xrightarrow{k_3}$ *carbonaceous deposites* could reproduce well the absorption curves of CH_4 and CD_4. Disappearance of the diffusion process in the kinctic equations was justified by extremely fast diffusion of hydrogen and remarkably slow diffusion of carbon into the bulk of Zr.

The kinetic isotope effects were measured from the analyses of absorption curves. The differences in the activation energies were evaluated to be $\Delta E_{k_1}(CD_4) - \Delta E_{k_1}(CH_4) = 7.7$ kJ.mol., whereas unacceptalbly large difference was obtained for $E_{k_2}(CD_4) - \Delta E_{k_2}(CH_4)$. As for k_3, it was concluded that no appreciable isotope effect appeared.

With respect to the isotope effect on k_1, the *ab inito* calculations could provide details of reaction mechanisms such as the structures of the adsorbed species and activated complex. It gave the differences in the activation energies for k_1 between CD_4 and CH_4 to be 4.78 kJ/mol. and the ratio of frequency factors, $\nu * (CH_4)/\nu * (CH_4)$, to be 1.37. This difference in the activation energy was quite close to that obtained from the experimental data and it was also true for the ratio of frequency factors. No appreciable isotope effect on k_3 was rationalized by the reactions among decomposition products such as $CQ_2(a)$, $CQ(a)$ and/or $C(a)$ (Q=H or D), On the other hand, the unacceptalble large isotope effect on k_2 was ascribed to insufficient accuracy of the first inflecting concave part in absorption curves.

References

[1] K. Watanabe, W. M. Shu, M. Motohashi, and M. Matsuyama, *Fusion Engn. Design*, 39/40 (1998) 1055 –1060

[2] L. C. Emerson, R. J. Knize, J. L. Cecchi, and O. Auciello, *J. Vac. Sci. Technol.*, A4 (1986) 297–299

[3] L. C. Emerson, R. J. Knize, and J. L. Cecchi, *J. Vac. Sci. Technol.*, A5 (1987) 2584–2586

[4] W. M. Shu, M. Matsuyama, and K. Watanabe, *Ann. Rept. HRC., Toyama Univ.*, 16 (1996) 59–68

[5] M. Matsuyama, E. Motohashi, W. M. Shu, and K. Watanabe, *Ann. Rept. HRC., Toyama Univ.*, 17 (1997) 73–84

[6] K. Watanabe, W. Shu, and M. Matsuyama, *Ann. Rept. Hydrogen Isot. Res. Centr.*, 26 (2006) 1–12

[7] M. J. Frisch, G. W. Trucks, H. B. Schlegel, G. E. Scuseria, M. A. Robband J. R. Cheesemanand J. A. Montgomeryand Jr.and T. Vrevenand K. N. Kudinand J. C. Burantand J. M. Millamand S. S. Iyengarand J. Tomasiand V. Baroneand B. Mennucciand M. Cossiand G. Scalmaniand N. Regaand G. A. Peterssonand H. Nakatsujiand M. Hadaand M. Eharaand K. Toyotaand R. Fukudaand J. Hasegawaand M. Ishidaand T. Nakajimaand Y. Hondaand O. Kitaoand H. Nakaiand M. Kleneand X. Liand J. E. Knoxand H. P. Hratchianand J. B. Crossand C. Adamoand J. Jaramilloand R. Gompertsand R. E. Stratmannand O. Yazyevand A. J. Austinand R. Cammiand C. Pomelliand J. W. Ochterskiand P. Y. Ayalaand K. Morokumaand G. A. Vothand P. Salvadorand J. J. Dannenbergand V. G. Zakrzewskiand S. Dapprichand A. D. Danielsand M. C. Strainand O. Farkasand D. K. Malickand A. D. Rabuckand K. Raghavachariand J. B. Foresmanand J. V. Ortizand Q. Cuiand A. G. Babouland S. Cliffordand J. Cioslowskiand B. B. Stefanovand G. Liuand A. Liashenkoand P. Piskorzand I. Komaromiand R. L. Martinand D. J. Foxand T. Keithand M. A. Al-Lahamand C. Y. Pengand A. Nanayakkaraand M. Challacombeand P. M. W. Gilland B. Johnsonand W. Chenand M. W. Wongand C. Gonzalezand, and J. A. Popleand, *Gaussian03, RevisionB.03*, Gaussian Inc.and Pittsburgh, 2003

[8] Y. Fukai, K. Tanaka and H. Uchida, *Suiso to Kinzoku* (in Japanese), p.115, Uchida Rokakuho Publishing Co., Tokyo, 1998

[9] The Japan Institute of Metals, *Metal Databook (2nd Ed.)* (in Japanese), p.29, Muruzen, Tokyo, 1984

[10] H. S. Carslaw and J. G. Jeager. *Conduction of Heat in Sollids (2nd Ed.)*, p.54, Clarendon Press, Oxford, 1959.

[11] R. Kiriyama and H. Kiriyama, *Kohzoh Muki Kagaku* I, p.59, Kyoritsu Shuppan (in Japanese), Tokyo, 1970

[12] L. Melander, *Isotope Effects on Reaction Rates*, p.44, Roland Press, New York, 1960